Chinese Chemical Letters 33 (2022) 2741–2746

Contents lists available at ScienceDirect

Chinese Chemical Letters

journal homepage: www.elsevier.com/locate/cclet

Fabrication of NiCoP decorated TiO_2/polypyrrole nanocomposites for the effective photocatalytic degradation of tetracycline

Yalu Wu, Yinyin Xu*, Yan Zhang, Jingbo Feng, Yuanyuan Li, Jiaying Lan, Xiuwen Cheng*

Key Laboratory for Environmental Pollution Prediction and Control, College of Earth and Environmental Sciences, Lanzhou University, Lanzhou 730000, China

ARTICLE INFO

Article history:
Received 22 June 2021
Revised 29 July 2021
Accepted 22 August 2021
Available online 26 August 2021

Keywords:
TiO_2
NiCoP
Polypyrrole
Visible light photocatalytic
Tetracycline

ABSTRACT

Due to the massive discharge of antibiotics in water, it is an urgent matter to remove antibiotics from waste water. The photocatalysts with high stability and activity have attracted extensive attention from researchers. By an *in-situ* polymerization method, polypyrrole (PPy) was modified on the surface of TiO_2 (named as TiO_2/PPy). By one-step reduction method, NiCoP was grafted on the surface of TiO_2/PPy (named as TiO_2/PPy/NiCoP) to synthesize the photocatalyst of TiO_2/PPy/NiCoP for degradation of tetracycline (TC) antibiotic. The characterization results revealed that NiCoP was deposited on the surface of TiO_2/PPy successfully. The photocatalytic experiment results illustrated that 83.2% of TC could be degraded at natural pH with 20 mg of TiO_2/PPy/NiCoP in 50 mL of TC solution (10 mg/L) under visible light irradiation. The high catalytic activity is attributed to the attachment of NiCoP on the surface of TiO_2/PPy which can enlarge the light response range of TiO_2 effectively. Scavenger studies revealed that the degradation of TC was dominated by $^{\bullet}O_2^-$ and h^+. The photodegradation efficiency of TC with TiO_2/PPy/NiCoP still reached over 74% after 5 consecutive cycles, indicating the potential applications in practical wastewater.

As an emerging class and ubiquitous occurrence of recalcitrant organic pollutants, pharmaceuticals and personal care products (PPCPs) have been heavily consumed in modern society [1]. The massive discharge of PPCPs in water and the corresponding risks to aquatic life and human, including antibiotic resistance, hormonal disruption and toxicity, has become a serious problem [2,3]. As reported, more and more PPCPs, including drugs (antibiotics, sedatives, antiepileptics, *etc.*), hormones (natural and synthetic), X-ray contrast agents, musk fragrance, *etc.* have been detected in varieties of the aquatic environment [4]. Because of the biologically cumulative effect at low concentration, PPCPs are recognized as the subject arising scientific interest and public concern. As a kind of extensive use in veterinary medicine and human, antibiotics get more attention than other kinds of PPCPs and have been widely used for the treatment of parasitic, fungal and bacterial infections [3,5].

As one type of antibiotics, tetracycline (TC) is a kind of natural or semi-synthetic broad-spectrum antibiotic produced by actinomycetes. Because of the resistance to a variety of Gram-positive bacteria and Gram-negative bacteria, TC is widely used in disease control, feed addition and promoting the growth of livestock and poultry [6]. However, about 50%-80% of antibiotics cannot be absorbed and are excreted into the soil and aquatic environment. This situation can induce environmental risks and lead to serious problems for human health [7]. Thus, the removal of TC from water solution is very important.

Recently, membrane, fenton oxidation, adsorption, electrochemical process and photocatalytic degradation, *etc.* have been introduced to remove tetracycline from water [8–11]. For example, Guo *et al.* had been synthesized a direct Z-scheme Ce@Fe core-shell nanotube array heterojunction which was used for the photocatalytic degradation of TC with high degradation efficiency, good stability and sustainable recycling capability [9]. Photocatalytic degradation is considered to be one of the most attractive methods to alleviate environmental problems, because it can directly convert solar energy into chemical energy [11]. So far, many photocatalytic nanocomposites such as TiO_2, g-C_3N_4, MoO_3 have been successfully developed and show great potential in energy conversion and environmental remediation [12–15]. As reported, a hollow nanotube Fe_2O_3/MoO_3 heterojunction had been prepared for the photoelectrocatalytic conversion of small-molecule alcohols [12]. Liu *et al.* synthesized a novel *Z*-scheme Fe_2O_3/g-C_3N_4 hybrid for CH_3OH oxidation to HCHO [15]. TiO_2 possesses excellent properties, such as long-term mechanical and thermal stability even un-

* Corresponding authors.
E-mail addresses: yyxu@lzu.edu.cn (Y. Xu), chengxw@lzu.edu.cn (X. Cheng).

https://doi.org/10.1016/j.cclet.2021.08.099
1001-8417/

der irradiation, corrosion resistance, nontoxicity, availability and low cost [16–18]. Therefore, it is widely used in photocatalytic degradation for pollutants. However, TiO_2 just only responds to the UV light due to its wide band gap, which limits the absorbable radiation. The low quantum efficiency of TiO_2 resulted in the low photocatalytic efficiency [18]. Some modification methods, such as element doping, noble metal modification, semiconductor composite, surface sensitization, can improve the response of TiO_2 to visible light and the photocatalytic activity [19,20]. It has been reported that many new TiO_2 complexes have been synthesized for adsorption and photocatalytic degradation. Some reports have improved the synthesis method of TiO_2 to make the synthesis process more convenient. For example, the latest synthesis of TiO_2/SiO_2-800 was prepared by Ji *et al.* [21]. At the same time, there are also many efficient photocatalysts, such as g-C_3N_4/TNTs, to realize the photocatalytic degradation of sulfamethazine [22]. Meanwhile, TNTs@ACF can efficiently degrade diclofenac under sunlight [23]. The above photocatalysts have a good degradation effect on PPCPs, however, the degradation of TC under visible light has not been reported. Due to the interface effect and local surface plasmon resonance (SPR) effect, it is another strategy to improve the efficiency of solar energy conversion to combine a suitable co-catalyst with a strong absorbing material [24]. The supported metal co-catalyst nanoparticles play an effective role in absorbing light, not only enhancing the absorption of visible light, resulting in more electron hole pairs, but also promoting the energy transfer to the conduction band of semiconductor.

As reported, the nanoparticles can be modified on the surface of photocatalyst to improve the separation efficiency of h^+ and e^-, and then significantly improve the photodegradation efficiency. The application of a suitable co-catalyst can expand the range of light absorption, promote the separation of holes and photogenerated electrons effectively and reduce the photocatalysis overpotential of the catalyst. As a new type of co-catalyst, transition metal phosphide (TMPS) which consists of transition metal and phosphorus elements has been studied and attracts the attention of researchers recently. With the advantages of low cost and high natural abundance, TMPS is an ideal choice to realize high-efficiency photocatalytic degradation [25]. TMPS is regarded as an excellent catalyst to replace precious metals. However, NiCoP shows low overpotential and charge transfer resistance, which indicates that the electrochemical performance of NiCoP is better than that of single metal phosphide [26]. NiCoP can provide more redox reaction sites through the synergistic effect between Ni and Co. At the same time, the participation of Ni can also improve the catalytic performance of Co [27]. Moreover, the presence of NiCoP co-catalyst can improve the transfer rate of photogenerated charge between materials [28]. The conductive polymer has excellent stability and easy synthesis, and can play a role similar to semiconductors due to its unique photoelectric properties [29]. Many conductive polymers can become good electron donors and electron transporters under visible light excitation, which can not only promote the separation of interface charges, but also can enhance the light absorption of semiconductor matrix [30,31]. They can be used as photosensitizers to modify wide band gap of inorganic semiconductors. As one of the conductive polymers, polypyrrole (PPy) with broadband absorption and high absorption rate for visible light has been widely used in biomaterials, supercapacitors and other fields due to its simple preparation and good environmental stability [30,32]. As a high mobility charge carrier, PPy can inhibit the recombination of electron hole pairs and improve the charge separation efficiency of photocatalysts [29]. As reported, PPy with unique structure has been widely used for the modification of semiconductors, such as BiOI/PPy and TiO_2/PPy, due to the convenient polymerization and modification on the surface of nanoparticles. Photocatalyst modified with PPy obtains stronger adsorption capacity, faster electron hole separation rate and higher light collection performance. Therefore, the photocatalytic activity of PPy modified photocatalyst can be improved significantly [31,33]. As reported, TiO_2/PPy had higher photocatalytic activity than that of original TiO_2 [34]. At the same time, photocatalyst modified with PPy shows excellent stability after repeated use and PPy is not be degraded in the process of photocatalysis. In addition, the abundant functional groups on PPy can also provide enough active sites for NiCoP loading [34].

Therefore, the TiO_2/PPy/NiCoP was prepared by sol-gel, *in-situ* polymerization and one-step chemical reduction method in this work. The prepared TiO_2/PPy/NiCoP would effectively improve the adsorption capacity and the visible-light photocatalytic activity. TC was selected to estimate the photodegradation activity of the synthesized TiO_2/PPy/NiCoP. The photocatalytic degradation mechanism was also studied.

The chemical reagents and instruments used in this work were shown in the Supporting information. Meanwhile, ultra-pure water was used throughout the experiment. TiO_2 was synthesized according to the published sol-gel method with some minor modifications [35]. The TiO_2/PPy was prepared by an *in-situ* polymerization method with minor modifications [36]. According to the literature, the TiO_2/PPy/NiCoP was synthesized by one-step chemical reduction method with some minor modifications [37]. The specific preparation process of TiO_2, TiO_2/PPy and TiO_2/PPy/NiCoP was illustrated in Supporting information.

The photocatalytic degradation experiments were carried out as a typical photocatalysis process. In a conical flask, some TiO_2/PPy/NiCoP nanocomposites were dispersed into 50 mL of TC solution at a certain concentration, which was followed by 30 min of mechanical stirring at 200 r/min and room temperature in the dark. Afterwards, a visible light source (300 W xenon lamp, HDL-II laboratory) was turned on to initiate the photocatalysis and the catalytic reaction was continuously stirred for 3 h. For analysis of TC, 2.5 mL of the suspension was transferred at a fixed time and filtered by a 0.22 μm of filter membrane to remove the catalyst. The concentration of TC was determined by a UV-vis spectrophotometer (UV-vis, EVO300 PC ultraviolet visible spectrophotometer, USA) at 354 nm. The catalyst dosage, concentration of pollutant solution, pH of pollutant solution, ionic strength of pollutant solution were investigated in the process of degradation TC with the same analytical procedure.

The transmission electron microscope (TEM, TECNAI G^2, FEI, USA) was conducted to characterize the size and morphology of TiO_2, TiO_2/PPy and TiO_2/PPy/NiCoP. The scanning electron microscope (SEM, JSM-6701F, Japan Jeol Ltd.) and X-ray energy dispersive spectrometer (EDS, Oxford instrument company, UK) were conducted to characterize the morphology and chemical composition of TiO_2/PPy/NiCoP. Fourier transform infrared spectra were determined on a NEXUS 670 FT-IR spectrometer (American Nicolet Company). The X-ray photoelectron spectroscopy (XPS, AXIS Ultra DLD, Shimadzu Institute, Japan) was conducted to characterize the photoelectron spectroscopy of TiO_2/PPy/NiCoP. The crystal structure of the prepared nanoparticles was characterized by the X-ray diffraction spectrometer (XRD, XRD-6000, Shimadzu, Japan). The optical properties of the materials were characterized by a UV-vis diffuse reflection spectroscopy (DRS) using a UV-visible NIR spectrophotometer (DRS, Lambda 950, PerkinElmer). The steady-state & time-resolved photoluminescence (PL, FLS920, USA) spectra was conducted to characterize the lifetime analysis of TiO_2, TiO_2/PPy and TiO_2/PPy/NiCoP.

The morphologies and chemical composition of the prepared nanocomposites were characterized by TEM, SEM and EDX (energy dispersive X-ray). As illustrated in Fig. 1A, the average diameter of the prepared TiO_2 was about 20-30 nm. The prepared TiO_2 was granular, highly crystalline, and agglomerated, which was consistent with the literature reported [38]. As for the TiO_2/PPy

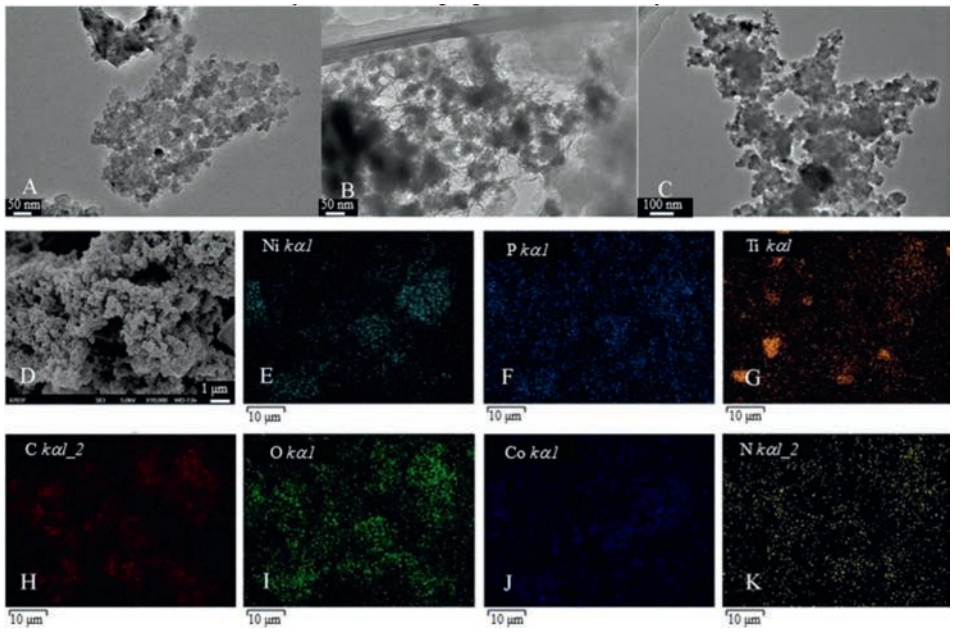

Fig. 1. TEM images of (A) TiO_2, (B) TiO_2@PPy and (C) TiO_2@PPy@NiCoP; SEM image of (D) TiO_2@PPy@NiCoP and the elemental mapping for (E) Ni, (F) P, (G) Ti, (H) C, (I) O, (J) Co, and (K) N of TiO_2@PPy@NiCoP.

(Fig. 1B), a layer of translucent PPy was attached to the surface of TiO_2 and did not affect the structure of TiO_2. The phenomenon indicated that the TiO_2/PPy was successfully synthesized. As can be seen from Figs. 1C and D, some black nanoparticles of NiCoP were grafted onto the surface of TiO_2/PPy and the morphology of TiO_2/PPy/NiCoP nanocomposites were relatively uniform. As shown in Figs. 1E–K, the EDS mapping images of TiO_2/PPy/NiCoP indicated the existence of Ni, P, Ti, C, O, Co and N elements in TiO_2/PPy/NiCoP. The above results confirmed that the TiO_2/PPy/NiCoP was prepared successfully.

The surface chemical composition of TiO_2/PPy/NiCoP was studied by XPS. The XPS spectra of TiO_2/PPy/NiCoP indicated that the sample consisted of nuclear energy levels of C 1s, N 1s, O 1s, Ti 2p, Ni 2p, Co 2p and P 2p (Figs. S1A–E in Supporting information), which proved that NiCoP had been successfully grafted on the surface of TiO_2/PPy. As displayed in Fig. S1F (Supporting information), the peaks of Ni at 855.7 and 873.35 eV were attributed to Ni $2p_{3/2}$ and Ni $2p_{1/2}$ of Ni^0, respectively [39]. The peaks at 861.7 and 880.05 eV for Ni were attributed to Ni $2p_{3/2}$ (Oxide) and Ni $2p_{1/2}$ (Oxide), respectively (Fig. S1F). As illustrated in Fig. S1G (Supporting information), the peaks at 781.45 and 797.05 eV for Co were assigned to Co $2p_{3/2}$ and Co $2p_{1/2}$ of Co^0, respectively [37]. As illustrated in Fig. S1H (Supporting information), the peak of P at 135.25 eV was attributed to P 2p of P^0 [40]. As shown in Fig. S1G (Supporting information), the peaks of Co at 786.05 and 803.2 eV were attributed to Co $2p_{3/2}$(Oxide) and Co $2p_{1/2}$(Oxide), respectively [37]. The above results illustrated that TiO_2/PPy/NiCoP had been synthesized successfully.

The qualitative and crystal structure of TiO_2, TiO_2/PPy, TiO_2/PPy/NiCoP were characterized by XRD. Seen from Fig. 2A, the peaks of 27.42°, 36.06° and 54.30° were sharp and obvious, which confirmed the good crystallinity of TiO_2 nanoparticles. The peaks at 25.30°, 37.72°, 39.20°, 48.08°, 54.30°, 62.72° and 69.00° were attributed to the anatase TiO_2 [41]. The peaks at 27.42°, 36.06°, 41.24°, 44.00°, 56.62°, 64.04° and 69.76° were attributed to the rutile TiO_2 [41]. As illustrated in Fig. 2A (curve b), the crystal structure of TiO_2 had no obvious change after being modified with PPy. The broad peak of PPy at 26° was not obvious as shown in the green box because of the coexistence of the sharp peak of TiO_2 [42]. It indicated that the synthesized PPy possessed an amorphous structure [43]. The diffraction peaks of NiCoP at 41.24°, 44.00° which were corresponded to the (111) and (201) crystal planes of NiCoP had some deviation from the standard card of NiCoP (PDF No. 71-2336) [37]. This phenomenon was mainly due to the mixed valence states of the Co and Ni ions [37].

Fig. 2B illustrated the FT-IR spectra of TiO_2, TiO_2/PPy, TiO_2/PPy/NiCoP. The broad band from 450 to 900 cm^{-1} in the green box of Fig. 2B (curve a) correspond to Ti-O-Ti and Ti-O stretching [44]. The peaks at 1625.7 cm^{-1} and 3434.6 cm^{-1} may be attributed to the bending and stretching vibration of hydroxyl or water molecules, which proved the successful preparation of TiO_2 [45]. The absorption peak at 1178.3 cm^{-1} was attributed to the specific characteristic peak of PPy according to the published literature [46]. It proved the successful synthesis of TiO_2/PPy. The band appearing in the green circle of Fig. 2B (curve c) was the characteristic absorption of Ni-P and Co-P bond in NiCoP, which proved the successful preparation of TiO_2/PPy/NiCoP [47].

The light adsorption properties of TiO_2, TiO_2/PPy and TiO_2/PPy/NiCoP in the wavelength coverage of 300-700 nm were investigated by DRS. As can be seen from Fig. 2C, TiO_2 only had strong absorption at the wavelength less than 400 nm, which was corresponded to the band gap of 2.8 eV. As calculated, the adsorption edge of TiO_2 was about 394 nm. The decrease of the band-gap for TiO_2 was mainly attributed to the existence of mixed crystal TiO_2. After being modified with PPy, the absorption wavelength of TiO_2/PPy was in the range of 200–700 nm (Fig. 2C, curve b). The absorption of TiO_2/PPy in the ultraviolet region was weaker than that of TiO_2, which was due to the modification of PPy on the surface of TiO_2. It might be caused a possible charge-transfer transition at the interface between TiO_2 and PPy, for the presence of PPy. The PPy may affect visible light diffuse reflection of TiO_2. The band gap of the PPy which was calculated by tauc plot was found to 2.0 eV. After modified with NiCoP, the absorption wavelength of TiO_2/PPy/NiCoP (Fig. 2C, curve c) ranged from 200 nm to 700 nm which was significantly higher than that of TiO_2/PPy. The above results showed that TiO_2/PPy/NiCoP could expand the light response to the visible light region, which was essential for improving photocatalytic performance.

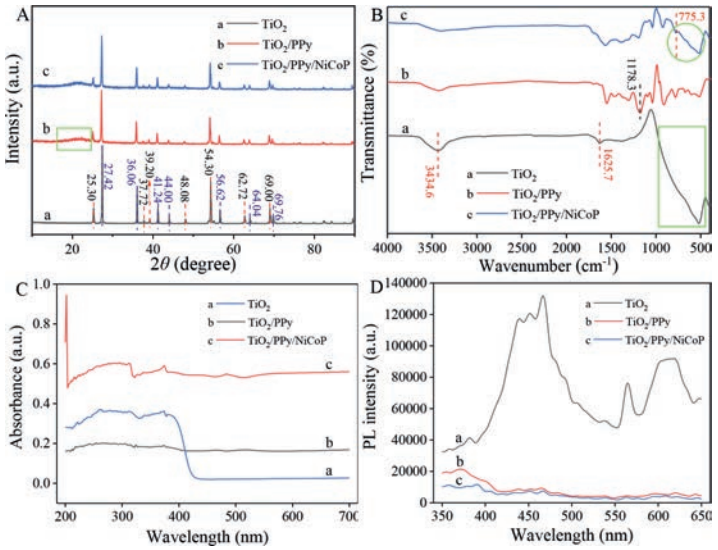

Fig. 2. (A) XRD pattern, (B) FT-IR spectra, (C) UV-vis-DRS spectra and (D) PL spectra of the prepared nanocomposites: (a) TiO_2 nanoparticles, (b) TiO_2/PPy and (c) TiO_2/PPy/NiCoP nanocomposites.

The PL spectra of TiO_2, TiO_2/PPy and TiO_2/PPy/NiCoP were presented in Fig. 2D. The photoluminescence intensity came from the recombination of free charge carriers in nanocomposites [48]. So, the decreasing of fluorescence intensity means that the semiconductor material has high carrier separation efficiency. As can be seen from Fig. 2D, TiO_2/PPy and TiO_2/PPy/NiCoP had lower PL intensity than TiO_2. This phenomenon indicated that the carrier separation ability in TiO_2/PPy/NiCoP was higher, which was more conducive to the photodegradation of TC.

The photocatalytic activities of the synthesized TiO_2/PPy/NiCoP were evaluated by the photocatalytic degradation of TC under visible light ($\lambda > 400$ nm). The effect of radiation time on the degradation efficiency of TiO_2/PPy/NiCoP was investigated. The experiments were carried out according to the following process. Firstly, 5 mg of TiO_2/PPy/NiCoP were added into 50 mL 10 mg/L of TC solution and was degraded under visible light for 0-9 h subsequently. Prior to irradiation, the above solution was oscillated for 30 min under dark conditions. As seen from Fig. S2 (Supporting information), the degradation efficiency of TC with TiO_2/PPy/NiCoP was increased gradually with the time lasting from 0 to 3 h. After 3 h later, the degradation efficiency of TC with TiO_2/PPy/NiCoP had no obvious change. As a result of that, 3 h was selected as the optimal reaction time in the following experiments. As shown in Fig. S2 (Supporting information), the photocatalytic degradation efficiency of 72.9% was higher than that of adsorption removal efficiency of 39.5% in dark with TiO_2/PPy/NiCoP lasting for 3 h. This phenomenon illustrated that the photocatalytic degradation of TiO_2/PPy/NiCoP under visible light could greatly improve the removal efficiency of TC from water solution.

The photocatalytic activity of TiO_2, TiO_2/PPy and TiO_2/PPy/NiCoP (10 mg) was investigated by the degradation of TC (50 mL, 10 mg/L). As shown in Fig. 3A, the photodegradation efficiency for TC with TiO_2/PPy/NiCoP nanocomposites was better than that of TiO_2 and TiO_2/PPy. The photocatalytic degradation efficiency of TiO_2/PPy/NiCoP for TC reached to 72.9%. This may be due to the improved photocatalytic performance of TiO_2 supported by NiCoP.

As reported, pH value of the aqueous solution can influence the photocatalytic degradation of contaminants. To study the effect of pH on the photocatalytic degradation efficiency of TiO_2/PPy/NiCoP for TC, 0.1 mol/L HCl and 0.1 mol/L NaOH were used to adjust the pH value of the aqueous solution. In this case, 10 mg of TiO_2/PPy/NiCoP were added into 50 mL TC solution (10 mg/L) with the pH ranged from 3 to 10. As seen from Fig. 3B, the photodegradation efficiency of TC by TiO_2/PPy/NiCoP was 45.6% with the aqueous solution pH 3 at 3 h. This phenomenon was attributed to the dissolution of NiCoP in the strong acid environment, which reduced the photocatalytic property of TiO_2/PPy/NiCoP. However, the photodegradation efficiency of TC with TiO_2/PPy/NiCoP had no obvious change with the pH values ranging from 4 to 10, which proved that the TiO_2/PPy/NiCoP had a relatively wide pH adaptation range. As can be seen from Fig. 3B, the high removal efficiency of TC was obtained at pH 5 with the removal rate at 73.1%, which was close to the removal rate of 72.9% at the natural pH value. This phenomenon illustrated that the prepared TiO_2/PPy/NiCoP had potential application value as a photocatalytic material to remove TC from the natural water solution. Therefore, natural pH was selected in the following experiment.

The influence of the initial concentration of TC on the photodegradation efficiency was investigated with 10 mg of prepared TiO_2/PPy/NiCoP at natural pH under visible light lasting for 3 h. As illustrated in Fig. 3C, the degradation efficiency of TC was increased from 65.7% to 89.1% with the concentration of TC increasing from 5 mg/L to 100 mg/L. This phenomenon illustrated that the increase of TC concentration could enhance the possibility of TC capture by TiO_2/PPy/NiCoP. However, the removal efficiency of TC was decreased significantly from 89.1% to 26.2% with the concentration of TC increasing from 100 mg/L to 200 mg/L. This phenomenon was attributed to the limitation of the TiO_2/PPy/NiCoP dosage, which led to the incomplete degradation of TC. Seen from Fig. 3C, 89.1% of TC could be removed with the concentration of TC at 100 mg/L. However, the concentration of TC in the natural environment was low-level (ng-μg/L) [49]. So, 10 mg/L of TC with a high degradation rate was selected in the following experiment.

To study the effect of ionic strength on the performance of TiO_2/PPy/NiCoP for the photocatalytic degradation of TC, 0.02–0.5 mol/L of NaCl were added to the reaction systems. As can be seen from Fig. 3D, the degradation efficiency of TC with TiO_2/PPy/NiCoP had no obvious change in the range of 0.02–0.5 mol/L of NaCl. As reported, the inorganic cations of Na^+ had no significant impacts on the photocatalytic process, because the hole or photogenerated electron was hardly utilized by the photocatalyst ascribing to the high oxidation state and stability [50,51]. Fig. 3D indicated that the inorganic anions of Cl^- had no obvious influence

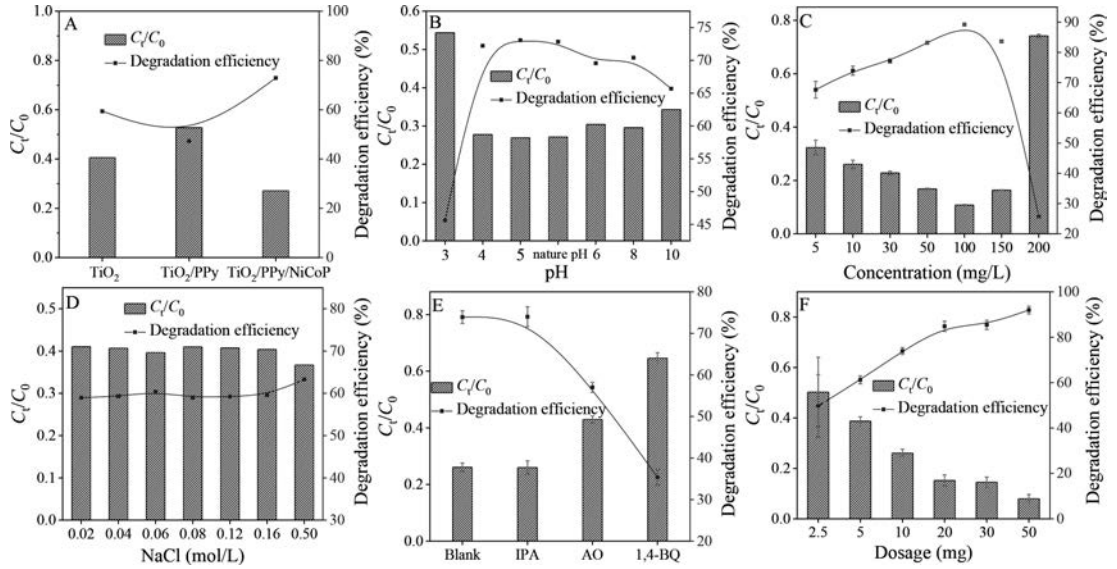

Fig. 3. Effect of (A) series photocatalysts, (B) initial pH of the aqueous solution, (C) TC concentration, (D) the ionic strength, (E) different scavengers and (F) the dosage of TiO_2/PPy/NiCoP on photocatalytic degradation of TC (room temperature, xenon lamp).

on the photodegradation efficiency of TC under visible light. This phenomenon illustrated that the TiO_2/PPy/NiCoP photocatalyst has a strong anti-interference ability and can be applied in real waste water.

In order to explore the possible mechanism and confirm the photo-produced active species, the trapping experiments were carried out as following. The active species capture agents of isopropanol (IPA), ammonium oxalate (AO) and 1,4-benzoquinone (1,4-BQ) were recommended to capture $^{\bullet}OH$, h^+ and $^{\bullet}O_2^-$, receptively [52]. At room temperature and natural pH, 1 mmol/L IPA, AO and 0.1 mmol/L 1,4-BQ were added into 50 mL TC (10 mg/L) with 10 mg of TiO_2/PPy/NiCoP, receptively. As can be seen from Fig. 3E, the removal efficiency of TiO_2/PPy/NiCoP for TC can reach to 72.9% without any quenchers. As illustrated in Fig. 3E, the photodegradation efficiency of TC has no obvious change after the addition of IPA into the solution. The results illustrated that $^{\bullet}OH$ was not the principal active species in the photocatalytic process. However, the photodegradation efficiency of TiO_2/PPy/NiCoP for TC decreased to 56.2% and 34% with the addition of 1 mmol/L of AO and 0.1 mmol/L of 1,4-BQ, which indicated that h^+ and $^{\bullet}O_2^-$ played prominent roles. Among those two radicals, $^{\bullet}O_2^-$ played the most crucial role in the photocatalytic degradation process, which illustrated that $^{\bullet}O_2^-$ was the main oxidative species responsible for the photocatalytic degradation of TC [52].

The effect of the dosage of TiO_2/PPy/NiCoP on the degradation of TC was also investigated at room temperature and natural pH with 50 mL 10 mg/L of TC. Seen from Fig. 3F, the photodegradation efficiency of TC increased gradually with the quality of TiO_2/PPy/NiCoP increasing. The photodegradation efficiency of TC reached up to 90.0% with 50 mg of TiO_2/PPy/NiCoP. This might be attributed to the abundant active species providing by TiO_2/PPy/NiCoP. The degradation efficiency of TC with 20 mg and 30 mg TiO_2/PPy/NiCoP was 83.2% and 84.0%, receptively. Considering the economy and effectiveness, 20 mg of TiO_2/PPy/NiCoP were used in the following experiments.

The mechanism of degradation TC with TiO_2/PPy/NiCoP was studied. As illustrated, $^{\bullet}O_2^-$ is the main active species responsible for the photocatalytic degradation of TC. The degradation mechanism of TC with TiO_2/PPy/NiCoP nanocomposites was shown in Fig. 4A. A mass of photogenerated electron-hole pairs were generated in the TiO_2/PPy/NiCoP under visible light irradiation. As reported in the literature, electrons could reduce O_2 to produce

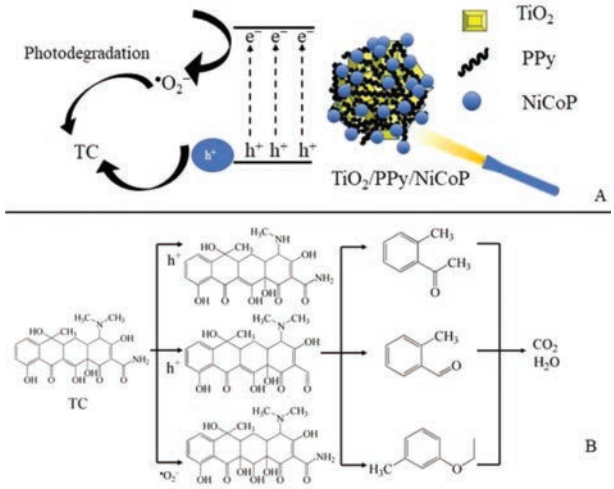

Fig. 4. (A) The degradation mechanism of TC with TiO_2/PPy/NiCoP. (B) Proposed intermediates and degradation routes of TC.

$^{\bullet}O_2^-$ [53]. The accumulated electrons in TiO_2/PPy/NiCoP could attract the dissolved O_2 and form $^{\bullet}O_2^-$, which could participate in the degradation of TC. The trapping experiments indicated that h^+ played the most crucial role in the photocatalytic degradation process. Under visible light, the accumulated h^+ of TiO_2/PPy/NiCoP could directly degrade TC [54]. Therefore, the improvement of the photocatalytic performance of TiO_2/PPy/NiCoP should be attributed to the synergy of $^{\bullet}O_2^-$ and h^+. The proposed intermediates and degradation routes of TC were shown in Fig. 4B. The degradation pathway of TC could be divided into four types as reported [53,55]. Seen from Fig. 4B, the unstable C-N bond of TC was broken under the action of h^+. Except for that, the -OH groups were taken off and the double bond was opened under the attack of $^{\bullet}O_2^-$. After the processes of demethylation, dehydroxylation, deamination and deamidation, TC would be decomposed into small molecules with only one benzene ring. And it eventually converted to CO_2, H_2O and other products. In order to verify the environmental friendliness of the products produced in the process of photodegradation, the hydroponic experiments of pea were carried out. The TC solution with the concentration of 10–50 mg/L before and after pho-

todegradation with TiO_2/PPy/NiCoP was used for the cultivation of peas. Before photodegradation with TiO_2/PPy/NiCoP, the germination rate of the peas in 50 mg/L of TC solution (Fig. S3b in Supporting information) was much lower than that of in 10 mg/L of TC solution (Fig. S3a in Supporting information) after cultivating for 1 day. After photodegradation with TiO_2/PPy/NiCoP, the germination rate of peas in the treating 50 mg/L (Fig. S3f in Supporting information) and 10 mg/L (Fig. S3e in Supporting information) of TC was much higher than that of the untreated TC solution for 1 day. After cultivation for 5 days, the growth of peas in the degradation solution in 50 mg/L (Fig. S3h in Supporting information) and 10 mg/L (Fig. S3g in Supporting information) of TC solution was better than that in the untreated 50 mg/L (Fig. S3d in Supporting information) and 10 mg/L (Fig. S3c in Supporting information) of TC solution. After photodegradation with TiO_2/PPy/NiCoP, the growth of peas in the 10 mg/L of TC solution was better than that in 50 mg/L of TC solution. The phenomenon illustrated that TC had a great influence on the growth of the plant and TiO_2/PPy/NiCoP could remove TC from water effectively. The dominant growth of peas in the treating TC solution illustrated that the photodegradation products of TC with TiO_2/PPy/NiCoP were friendly to the environment.

The reusability and stability of TiO_2/PPy/NiCoP were important properties for practical application. Under the same conditions, the reusability and stability of TiO_2/PPy/NiCoP were investigated by applying five repeated experiments. After the photocatalytic degradation experiment, the TiO_2/PPy/NiCoP were washed with ethanol and water alternately to remove surface-trapped organic compounds and then dried in the oven before application for another cycle. As can be seen from Fig. S4 (Supporting information), the degradation efficiency of TC with TiO_2/PPy/NiCoP was ranged from 74.3% to 83.2% with high photocatalytic activity after being reused for 5 times. The result illustrated that TiO_2/PPy/NiCoP consistently remained high photocatalytic performance and showed potential applications in photodegradation of TC in wastewater.

In summary, TiO_2/PPy/NiCoP were synthesized by an *in-situ* polymerization and one-step chemical reduction method. The characterization results illustrated that TiO_2/PPy/NiCoP had been successfully prepared. Under the visible light, the TiO_2/PPy/NiCoP obtained outstanding photocatalytic activity for TC with the degradation efficiency of 83.2% at nature pH with 20 mg of TiO_2/PPy/NiCoP nanocomposites in 50 mL TC (10 mg/L) solution. The photocatalytic results illustrated that the TiO_2/PPy/NiCoP photocatalyst obtained strong anti-interference ability, wide pH adaptation range and could be applied in real water samples. Furthermore, the reused experiments indicated that TiO_2/PPy/NiCoP possessed good reusability and stability with no significant reduction of the degradation efficiency after 5 cycles. Scavenger studies illustrated that the TC degradation was dominated by $^{\bullet}O_2^-$ and h^+. The probable degradation pathways of TC indicated that decarboxylation, hydroxylation, and demethylation were involved in the degradation. The newly developed visible-light-driven TiO_2/PPy/NiCoP photocatalyst was found to be a suitable candidate without noble metal for degradation of TC for practical application.

Declaration of competing interest

The authors declare no conflict of interest.

Acknowledgments

The authors are grateful for financial support from the National Natural Science Foundation of China (No. 41603087), Natural Science Foundation of Gansu (No. 20JR5RA282).

Supplementary materials

Supplementary material associated with this article can be found, in the online version, at doi:10.1016/j.cclet.2021.08.099.

References

[1] J.B. Ellis, Environ. Pollut. 144 (2006) 184–189.
[2] F.A. Caliman, M. Gavrilescu, Clean Soil Air Water 37 (2009) 277–303.
[3] J. Liu, M. Wong, Environ. Int. 59 (2013) 208–224.
[4] S. Suárez, M. Carballa, F. Omil, J.M. Lema, Rev. Environ. Sci. Biotechnol. 7 (2008) 125–138.
[5] B. Appavu, S. Thiripuranthagan, S. Ranganathan, E. Erusappan, K. Kannal, Ecotoxicol. Environ. Saf. 151 (2018) 118–126.
[6] T. Jing, J. Niu, H. Xia, et al., J. Sep. Sci. 34 (2011) 1469–1476.
[7] K. Kumar, S.C. Gupta, S.K. Baidoo, Y. Chander, C.J. Rosen, J. Environ. Qual. 34 (2005) 2082–2085.
[8] Y. Xu, T. Liu, Y. Zhang, et al., J. Mater. Chem. A 5 (2017) 12001–12014.
[9] S. He, C. Yan, X. Chen, et al., Appl. Catal. B: Environ. 276 (2020) 119138.
[10] C. Jiang, L. Liu, J. Crittenden, Front. Environ. Sci. Eng. 10 (2016) 1–8.
[11] Y. Zhou, J. He, J. Lu, Y.D. Liu, Y.B. Zhou, Chin. Chem. Lett. 31 (2020) 2623–2626.
[12] S. Huang, T. Ouyang, B. Zheng, M. Dan, Z. Liu, Angew. Chem. Int. Ed. 60 (2021) 9546–9552.
[13] X. Chen, L. Liu, P. Yu, Y. Mao, Science 331 (2011) 746–750.
[14] B. Lin, H. Li, H. An, et al., Appl. Catal. B: Environ. 220 (2018) 542–552.
[15] S. Huang, B. Zheng, Z. Tang, et al., Chem. Eng. J. 422 (2021) 130086.
[16] C. Pirola, D.C. Boffito, S. Vitali, C.L. Bianchi, J. Coat. Technol. Res. 9 (2012) 453–458.
[17] R. Guo, L. Nengzi, Y. Chen, et al., Chin. Chem. Lett. 31 (2020) 2661–2667.
[18] H.S. Mona, J. Farima, M. Afshan, H. Nasim, Catal. Sci. Technol. 8 (2018) 4044–4051.
[19] N. Pugazhenthiran, S. Murugesan, S. Anandan, J. Hazard. Mater. 263 (2013) 541–549.
[20] C. Huang, Y. Lv, Q. Zhou, et al., Ceram. Int. 40 (2014) 7093–7098.
[21] H. Ji, W. Liu, F. Sun, et al., Chem. Eng. J. 419 (2021) 129605.
[22] H. Ji, P. Du, D. Zhao, et al., Appl. Catal. B: Environ. 263 (2020) 118357.
[23] C. Dang, F. Sun, H. Jiang, et al., J. Hazard. Mater. 400 (2020) 123225.
[24] Q. Chen, X. Cheng, H. Long, Y. Rao, Chin. Chem. Lett. 31 (2020) 2583–2590.
[25] P. Ye, X. Liu, J. Iocozzia, et al., J. Mater. Chem. A 5 (2017) 8493–8498.
[26] Y. Wei, X. Zhang, Z. Wang, et al., Chin. Chem. Lett. 32 (2021) 119–124.
[27] J.K. Das, A.K. Samantara, S. Satyarthy, C.S. Rout, J.N. Behera, RSC Adv. 10 (2020) 4650–4656.
[28] Z. Xu, C. Du, H. Yang, et al., Chem. Eng. J. 421 (2020) 127871.
[29] V. Balakumar, A. Baishnisha, Surf. Interfaces 23 (2021) 100958.
[30] F. Deng, L. Min, X. Luo, S. Wu, S. Luo, Nanoscale 5 (2013) 8703–8710.
[31] S. Zheng, C. Zhang, Y. Ma, et al., Ceram. Int. 47 (2021) 10574–10581.
[32] Y. Wu, L. Shen, C. Zhang, et al., Desalination 505 (2021) 114766.
[33] L. Ding, X. Zhao, Y. Huang, et al., J. Colloid Interface Sci. 595 (2021) 168–177.
[34] Y. Li, S. Yan, X. Jia, et al., Appl. Catal. B: Environ. 287 (2021) 119926.
[35] C. Wu, K. Huang, J.M. Chern, Ind. Eng. Chem. Res. 45 (2006) 2040–2045.
[36] S. Lin, Y. Xu, X. Li, J. Ma, Desalin. Water Treat. 160 (2019) 343–353.
[37] Y. Wen, J. Qi, D. Zhao, et al., Appl. Catal. B: Environ. 293 (2021) 120196.
[38] Y. Zhang, H. Gan, G. Zhang, Chem. Eng. J. 172 (2011) 936–943.
[39] N. Cao, L. Yang, C. Du, et al., J. Mater. Chem. A 2 (2014) 14344–14347.
[40] R.Z. Jiang, D.T. Tran, J.P. McClure, D. Chu, ACS Catal. 4 (2014) 2577–2586.
[41] D. Nina, D. Marwa, M. Tzonka, et al., RSC Adv. 9 (2019) 2073–2080.
[42] M. Bhaumik, A. Maity, V.V. Srinivasu, M.S. Onyango, J. Hazard. Mater. 190 (2011) 381–390.
[43] Y. Chen, Y. Li, H. Wang, M. Yang, Carbon 45 (2007) 357–363.
[44] H. Khan, M.G. Rigamonti, D.C. Boffito, Appl. Catal. B: Environ. 252 (2019) 77–85.
[45] L. Yang, X. Bai, J. Shi, et al., Appl. Catal. B: Environ. 256 (2019) 117759.
[46] B.J.S. Johnson, J.H. Wolf, A.S. Zalusky, M.A. Hillmyer, Chem. Mater. 16 (2004) 2909–2917.
[47] S. Zhang, L. Song, X. Wu, Ceram. Int. 40 (2014) 5339–5342.
[48] M. Zhu, Q. Liu, W. Chen, et al., ACS Appl. Mater. Interfaces 9 (2017) 38832–38841.
[49] G.R. Boyd, H. Reemtsma, D.A. Grimm, S. Mitra, Sci. Total Environ. 311 (2003) 135–149.
[50] X. Yi, S. Ma, X. Du, et al., Chem. Eng. J. 375 (2019) 121944.
[51] C. Wang, L. Zhu, M. Wei, P. Chen, G. Shan, Water Res. 46 (2012) 845–853.
[52] H. Zhao, X. Liu, Y. Dong, et al., Appl. Catal. B: Environ. 256 (2019) 117872.
[53] X. Wei, H. Feng, L. Li, et al., Appl. Catal. B: Environ. 260 (2019) 118218.
[54] F. Chen, Q. Yang, X. Li, et al., Appl. Catal. B: Environ. 200 (2017) 330–342.
[55] Q. Zhu, Y. Sun, F. Na, et al., Appl. Catal. B: Environ. 254 (2019) 541–550.